Dimensionless Heat Transfer Correlations for Estimating Edge Heat Loss in a Flat Plate Absorber

Author: Nwosu, P.N., Ph.D
Affiliation: Energy Research Centre, University of Nigeria, Nsukka, and Department of Mechanical and Aeronautical Engineering, University of Pretoria, South Africa
Phone: +27-7031676565
e-mail: paul.nwosu@up.ac.za

Abstract

Data obtained from heat transfer relations discretized with the finite element method were used in developing dimensionless correlations, which led to determining prediction equations for the average edge temperature of a flat plate absorber. For a prescribed flux, if parameters like the incident radiation intensity, edge insulation thermal conductivity and ambient temperature are known, the value of the edge temperature variable is immediately determined. A range of edge-to-absorptive area ratios are considered, as well as the effects of the edge insulation on enhancing thermal performance. Notably, the edge loss is high in absorbers with small edge-to-absorptive area ratios and ambient conditions with low h_a and T_a.In extreme operating conditions however, the loss can be of a high proportion. As a result, edge insulation can be employed as a heat transfer enhancement feature to minimize useful energy losses, as well enhance steady-state heat transfer.

Keywords: edge heat loss; dimensionless groups; flat-plate absorber

1.0 INTRODUCTION

Edge heat transfer in absorbers with a planar configuration, uniformly irradiated from the top and with bottom insulation, is required in some energy conversion devices which find application in micro-batteries and miniature heat exchangers. Edge heat loss refers to useful heat loss emanating from the edges of an absorber plate. In relation to flat plate absorbers cooled from the edges, the heat dissipation characteristics and the resulting temperature profile are important in effectively monitoring the thermal performance of the plate in conditions which vary continuously. There are numerous applications for edge cooling of flat-plates in metallurgy, and electronic gadgets, etc. There are other application areas involving a plate with a heat absorbing surface, bottom and edge insulation - for instance, solar absorbers. In the case of solar absorbers, the edge loss is not desired since the thermal efficiency can be affected adversely, for this reason appropriate insulation measures are required. Although there are various insulation materials, the amount of insulation provision required to achieve a desired temperature range at the edges, and other points in the plate for a case of localized heating and cooling process, requires modeling of the relevant thermal

interaction. A key step in identifying and assessing the heat absorption and dissipation potential of typical energy conversion components is to develop models based on operational and ambient characteristics.

A number of studies have been undertaken to model the edge loss effects in flat absorbers however these studies are few [1, 2]. Many approaches have been adopted in the analysis of uniformly heated plates, some notable works include [3, 4]. There are some numerical studies in relation to thermal performance analysis of solar absorbers [5-7]. Although these are a fundamental attempt, the models are relatively inadequate to account for the edge loss. Few numerical studies have also been conducted vis-à-vis the edge loss, owing ostensibly to the complexity involved in modelling the edge loss. The evaluation of the edge loss is complicated as noted in [3] and hence the trivial edge loss coefficient recommended in the work. The effect of edge heat loss on the absorbers has not been given proper attention in the literature and there is poor design information on the improvement of absorbers regarding the edge insulation effects thus resulting in some suboptimal designs. At micro-level, proper thermal insulation measures become a challenge [5], consequently there is need to develop appropriate correlations so as to predict the influence of various fundamental variables and thermal loads.

The specification of the quality of insulation required to achieve a desired thermal efficiency and the evaluation of the heat extraction rate from the edge surface for the case of rapidly cooled edges, are crucial in designing absorbers which can efficiently perform in widely varying conditions. In this work, a numerical treatment based on the Galerkin finite element method is applied to the physical problem. This involves a stepwise formulation and development of the system equations. Also, this numerical method has the versatility to model complex geometries other than the regular rectangular flat plate when compared to other numerical methods [8, 9]. In addition, some unique dimensionless parameters governing the behaviour of the problem were identified, and prediction equations based on these dimensionless parameters were obtained.

2.0 PROBLEM STATEMENT

The two-dimensional finite element discretization of the differential element of the absorber plate with mutually perpendicular lines of heat flow is considered. If the absorber is uniformly irradiation, the bottom housing of the air heater is perfectly insulated and convection is the dominant mode of heat transfer, the equation for conservation of heat flux in the differential element of the absorber shown in Figure 1 is written as

$$\tau\alpha I dydx + q_x tdy + q_y tdx = \left(q_x + \frac{\partial q_x}{\partial x}dx\right)tdy + \left(q_y + \frac{\partial q_y}{\partial y}dy\right)tdx + h_f\left(T - T_f\right)dydx + U_t(T - T_a)dydx \quad (1)$$

where U_t for a two-cover heater is defined as

$$U_t = \frac{1}{\frac{1}{h_{c_1}} + \frac{1}{h_{c_2}} + \frac{1}{h_a}} \quad (2)$$

The finite element is employed in dicretization of the above equation since this represents a boundary value problem. The finite element envisions the solution region of the problem as built up of many small, inter-connected elements. The rectangular element is used to represent the rectangular domain. This will enable us determine the state variable(s) and the edge heat flux at specific boundaries using a system of nodes. Applying the conditions that must be satisfied by each interpolation function at each node, the interpolation functions which guarantee convergence for the element are given as [9]

$$\begin{aligned} N_1(r,s) &= \frac{1}{4}(1-r)(1-s) \\ N_2(r,s) &= \frac{1}{4}(1+r)(1-s) \\ N_3(r,s) &= \frac{1}{4}(1+r)(1+s) \\ N_4(r,s) &= \frac{1}{4}(1-r)(1+s) \end{aligned} \quad (3)$$

where *r* and *s* are the normalized co-ordinates of the elements. Modelization of the edge loss requires a detailed knowledge of the thermal interaction within the absorber, as well as with

its physical boundary. In the Galerkin finite element method [9], a residual integral equation corresponding to the differential equation is defined, consequently equation (1) after simplification is expressed as

$$\iint_A N_i(x,y)\left[\frac{\partial}{\partial x}\left(tk_x\frac{\partial T}{\partial x}\right)+\frac{\partial}{\partial y}\left(tk_y\frac{\partial T}{\partial y}\right)+\tau\alpha I-h_f\left(T-T_f\right)-U_t\left(T-T_a\right)\right]dA=0$$

$$i = 1, M \tag{4}$$

the above equation can be expressed more succinctly

$$\iint_A\left(k_x\left[\frac{\partial N}{\partial x}\right]^T\left[\frac{\partial N}{\partial x}\right]+k_y\left[\frac{\partial N}{\partial y}\right]^T\left[\frac{\partial N}{\partial y}\right]\right)\{T\}\,tdA+\iint_A h_f\left[N\right]^T\left[N\right]\{T\}\,dA+\iint_A U_t[N]^T\left[N\right]\{T\}\,dA$$
$$=\iint_A\tau\alpha I\left[N\right]^T dA+\iint_A h_f T_f\left[N\right]^T dA+\iint_A UT_a\left[N\right]^T dA-t\int q_\Omega n_\Omega\left[N\right]^T d\Omega \tag{5}$$

subject to the following

$$\Delta x_{ins}>0,\ k_{ins}>0\ and\ U_e=\frac{k_{ins}\gamma}{\Delta x_{ins}}$$
$$\Delta x_{ins}=0,\ k_{ins}=0\ and\ U_e=h_a \tag{6}$$

where $\left[N\right]^T$ is the M x 1 column matrix of interpolation functions, $\left[N\right]$ is the row matrix of interpolation functions with their differentials expressed above and $\{T\}$ is the column matrix (i.e. vector) of nodal temperatures. Equation (5) is of the form

$$\left[k^{(e)}\right]\{T\}=\left\{f_{ar}^{(e)}\right\}+\left\{f_h^{(e)}\right\}+\left\{f_U^{(e)}\right\}+\left\{f_{\Omega_{eg}}^{(e)}\right\} \tag{7}$$

The equation above represents a system of M equations for the two-dimensional finite element problem consisting of the absorber model with appropriate boundary conditions obtained via the Galerkin method. The left-hand side of equation (5) includes the temperature unknowns T, while the right-hand side is composed of forcing functions: solar flux, surface heat convection, top heat loss contribution, and the boundary heat flux for elements subject to

the edge loss on the boundary of the problem domain. The conductance $\left[k^{(e)}\right]$ in the above equation is defined as

$$\left[k_{eg}^{(e)}\right] = \iint_A \left(k_x \left[\frac{\partial N}{\partial x}\right]^T \left[\frac{\partial N}{\partial x}\right] + k_y \left[\frac{\partial N}{\partial y}\right]^T \left[\frac{\partial N}{\partial y}\right] \right) t dA + h_f \iint_A \left[N\right]^T \left[N\right] dA + U_t \iint_A [N]^T \left[N\right] dA + \int_{\Omega edge} U_{edge} \left[N\right]^T \left[N\right] t d\Omega_{edge} \tag{8}$$

The forcing functions in equation (7) are expressed as

$$\left\{f_{ar}^{(e)}\right\} = \iint_A \tau\alpha I \left[N\right]^T dA = \iint_A \tau\alpha I \left\{N\right\} dA$$

$$\left\{f_{h}^{(e)}\right\} = \iint_A h_f T_f \left[N\right]^T dA = \iint_A h_f T_f \left\{N\right\} dA$$

$$\left\{f_{U}^{(e)}\right\} = \iint_A U_t T_a \left[N\right]^T dA = \iint_A U_t T_a \left\{N\right\} dA$$

$$\left\{f_{eg}^{(e)}\right\} = \int_{\Omega edge} U_e T_a \gamma \left[N\right]^T t d\Omega_{edge} = \int_{\Omega edge} \frac{k_{ins} T_a}{\Delta x_{ins}} \gamma \left[N\right]^T t d\Omega_{edge} \tag{9}$$

where

$$\gamma = \frac{h_a \Delta x_{ins}}{h_a \Delta x_{ins} + k_{ins}}$$

The assembly of the element matrix equations has been implemented in a recent work [11] according to the topological configuration of the elements after the equations were transformed to global co-ordinates. The essential boundary conditions were introduced to obtain a condensed global matrix. The solution of the global equation was obtained after the assembly of the individual element equations using the matrix inversion technique so as to determine the nodal temperatures and associated fluxes. To determine the relative contributions of the relevant operational and ambient parameters, the following dimensionless groups are defined:

$$\bar{A}_e = \frac{A_e}{A_p}; \qquad \bar{T}_p = \frac{T_{e_{(av)}}}{T_f}$$

$$\phi_{edge} = \frac{q_{e_{loss}}}{\tau\alpha I A_p}; \hat{T} = \frac{T_a}{T_f}$$

$$\bar{\kappa} = \frac{k_{ins}\Delta x_{ins}}{kt}; \quad \bar{T}_i = \frac{T_i}{T_f} \tag{11}$$

The equations above which contain heat transfer rate expressions are essentially ratios of heat output to input in the system. The output comprises the heat loss, $q_{e_{loss}}$ .The input is the absorbed solar radiation. The ratio ϕ_{edge} is indicative of the amount of absorbed energy that is dissipated as edge heat loss. $\hat{T}$ gives an indication as to how the ambient temperature exceeds the fluid entrance temperature, and $\bar{T}_i$ is the non-dimensional nodal temperature values. $\bar{\kappa}$ gives the relative change in the value of the thermal conductivity of edge insulation. Once the primary variables (i.e. the temperature unknowns) have been determined, an appropriate flux equation can then be employed to obtain the edge loss.

The edge heat flux equation for an element is given as

$$q_{loss}^{(e)} = \int_{\Omega_{edge}} U_e \left(T^{(e)} - T_a\right) t d\Omega_{edge} \tag{12}$$

Assuming constant conditions, the edge heat flux equation can be expressed

$$q_{e_{loss}} = U_e A_e \left(T_{e(av)} - T_a\right) \tag{13}$$

where

$$A_e = 2.t.\left(L_p + W_p\right)$$

A_e is the edge area of absorber plate. The total convective heat flow rate from the physical absorber is the sum total of the convective heat flux components of all the elements employed in the finite element mesh of the absorber giving an indication of the heat transfer between the solid body and the fluid stream. Consequently, for an absorber with no edge insulation provision, the above equation is further simplified to get

$$q_{e_{loss}} = h_a A_e \left(T_{e(av)} - T_a \right) \tag{14}$$

The average edge temperature of the absorber $T_{e(av)}$ is obtained from the temperature values of the edge nodes congruent with the thermally active boundary. Combining equations (11) and (12), the following normalized equation is obtained

$$\phi_{egde} = \frac{U_e}{\tau\alpha I} \bar{A}_e T_f \left(\bar{T}_p - \hat{T} \right) \tag{15}$$

where $\bar{A}_e$ is the area ratio. Given the dimensionless relations above, the element 'stiffness' equation (8), is re-expressed as

$$\left[k_{eg}^{(e)} \right] = \iint_A \left(\left[\frac{\partial N}{\partial x} \right]^T \left[\frac{\partial N}{\partial x} \right] + \left[\frac{\partial N}{\partial y} \right]^T \left[\frac{\partial N}{\partial y} \right] \right) \left(\bar{h} \right)^2 ktdA + \bar{h} h_a \iint_A \left[N \right]^T \left[N \right] dA + U_t \iint_A [N]^T \left[N \right] dA$$
$$+ \int_{\Omega edge} \frac{\bar{\kappa} kt}{\Delta x_{ins}} \gamma \left[N \right]^T \left[N \right] td\Omega_{edge} \tag{16}$$

where $$\gamma = \frac{1}{1 + \bar{h}\bar{k}\left(\frac{k}{k_{ins}} \right)^2}$$

Depending upon the physical nature of the problem, the intricacy of the solution scheme may involve the definition of the domain, both physically and geometrically, the

domain could be bounded or unbounded as in this case. The approximations used in defining the physical characteristics of the domain are largely real world-oriented.

3.0 Dimensional Analysis

In order to obtain prediction equations for the edge heat loss from the absorber, dimensional analysis is employed. This involves determining the functional relationship between the various variables in the system by nondimensionally combining them into *dimensionless groups* or *products*. There are importantly two approaches which can be employed [12]: the Buckingham pi and the Raleigh methods. In the Buckingham pi method, a fundamental approach to it is to replace a list of system of variables with a finite number of dimensionless groups. The Buckingham pi method uses the symbol π to represent a dimensionless group (or product). The theorem is based on the idea of dimensional homogeneity. The Raleigh method is straightforward in comparison, for the resultant system of simultaneous equations involved is solved only once. The Raleigh method does not incorporate the pi notation. It simply, first, obtains a functional relationship between all the system variables, solves the system of equations determines the relevant dimensionless group(s). Thus predictive equations can then be obtained from the dimensionless products.
The procedure of the Raleigh method is given in [12], and it is applied in this work to obtain the dimensionless groups for the edge heat loss variable, $T_{e(av)}$. Employing this, the functional relationship between the average absorber temperature $T_{e(av)}$ and the relevant system variables is defined by

$$T_{e(av)} = T_{e(av)}(k_{ins}, k, h_a, h_f, T_a, T_f, \Delta x_{ins}, I) \tag{17}$$

$T_{e(av)}$ is the undetermined function. Following the systematic procedure of the Raleigh method, the above equation yields

$$T_{e(av)} = C_1 k_{ins}^{a1} k^{a2} h_a^{a3} h_f^{a4} T_a^{a5} T_f^{a6} \Delta x_{ins}^{a7} I^{a8} \tag{18}$$

where are $a_1, a_2, a_3, ...a_7$ are exponents assigned to the physical quantities. In terms of the fundamental dimensions M,L,T and t, the above equation can be expressed as

$$(T) = C_1\left(MLt^{-3}T^{-1}\right)^{a1}\left(MLt^{-3}T^{-1}\right)^{a2}\left(Mt^{-3}T^{-1}\right)^{a3} \left(Mt^{-3}T^{-1}\right)^{a4}(T)^{a5}(T)^{a6}(L)^{a7}\left(Mt^{-3}\right)^{a8} \quad (19)$$

Solving analytically, the following equation is obtained

$$\frac{T_{e(av)}k_{ins}^2}{\Delta x_{ins}^2 I\, h_f}. = C_1\left(\frac{k}{k_{ins}}\right)^{a_2}\left(\frac{h_a \Delta x_{ins}}{k_{ins}}\right)^{a_3}\left(\frac{k_{ins}T_a}{\Delta x_{ins} I}\right)^{a_5}\left(\frac{k_{ins}T_f}{\Delta x_{ins} I}\right)^{a_6} \quad (20)$$

Since there are eight variables and four fundamental dimensions, then four dimensionally homogenous groups appear on the right-had side of the above equation. In order to obtain values of the ambient parameters on a temporal basis, typically a weather logger is used in recording the variation (Fig. 2), hence average values can then be calculated. Simulation results were obtained using results from the finite element formulation and employing typical operational and ambient. Table 1 gives the data obtained from the simulation results considering various combinations of the operational variables and the use parameters of the absorber. It also shows the various groups of the obtained data with the corresponding exponent. The evaluation of the exponents appearing in the foregoing entails correlating the data in Table 1 with the dimensionless groups obtained in (20). In the table, consideration is given to a range of edge insulation conductivities, k_{ins}. The lowest k_{ins} value (k_{ins} = 0.01 W/mK) given in Group 1 of the table represents excellent edge insulation. k_{ins} = 0.1 W/mK (Group 2), implies low-grade insulation. k_{ins} = 50 W/mK (Group 3), represents very poor insulation. The three groups of data shown in the table gives the average values of the dimensionless product $\left(\frac{T_{e(av)}k_{ins}^2}{It_{ins}^2 h_f}\right)\left(\frac{h_a t_{ins}}{k_{ins}}\right)^{-1}$. Since the values of the three groups differ on account of k_{ins}, it becomes tenable to have three different dimensionless equations to represent the various groups.

To obtain the exponents of the dimensionless groups, the results are solved analytically for each group in the table. The dimensionless groups with exponents a_2, a_5 and a_6 in equation (20) are constant. Then equation (20) becomes

$$\frac{T_{e(av)}k_{ins}^2}{\Delta x_{ins}^2 I\, h_f} = C_1\left(\frac{h_a \Delta x_{ins}}{k_{ins}}\right)^{a_3} \quad (21)$$

Considering two data points in any of the test groups in the table (say 3 and 5), these data points can be used to determine the exponent , a_3 in the equation above and in each group. Substituting data points into equation (21)

$$\left.\frac{T_{e(av)}k_{ins}^2}{\Delta x_{ins}^2 I\, h_f}\right|_3 = C_1\left.\left(\frac{h_a \Delta x_{ins}}{k_{ins}}\right)^{a_3}\right|_3 \tag{22}$$

and

$$\left.\frac{T_{e(av)}k_{ins}^2}{\Delta x_{ins}^2 I\, h_f}\right|_5 = C_1\left.\left(\frac{h_a \Delta x_{ins}}{k_{ins}}\right)^{a_3}\right|_5 \tag{23}$$

Dividing (23) by (22)

$$\frac{\left.\frac{T_{e(av)}k_{ins}^2}{\Delta x_{ins}^2 I\, h_f}\right|_5}{\left.\frac{T_{e(av)}k_{ins}^2}{\Delta x_{ins}^2 I\, h_f}\right|_3} = \left(\frac{\left.\left(\frac{h_a \Delta x_{ins}}{k_{ins}}\right)\right|_5}{\left.\left(\frac{h_a \Delta x_{ins}}{k_{ins}}\right)\right|_3}\right)^{a_3} \tag{24}$$

and taking the natural logarithm of the above equation:

$$a_3 = \frac{\ln\left[\left(T_{e(av)}k_{ins}^2 / \Delta x_{ins}^2 I\, h_f\right)_5 / \left(T_{e(av)}k_{ins}^2 / \Delta x_{ins}^2 I\, h_f\right)_3\right]}{\ln\left[\left(h_a t_{ins} / k_{ins}\right)_5 / \left(\left(h_a t_{ins} / k_{ins}\right)\right)_3\right]} \tag{25}$$

To evaluate a_3 for the three groups, the average values of the dimensionless expressions from Table 1 are substituted into equation (25) to obtain: a_3 =-0.0001 for groups 1 and 2, and a_3 =-0.001,for group 3.Substituting these values into (21), for groups 1 and 2, yields

$$\frac{T_{e(av)}k_{ins}^2}{\Delta x_{ins}^2 I\, h_f} = C_1\left(\frac{h_a \Delta x_{ins}}{k_{ins}}\right)^{-0.0001} \tag{26}$$

and for group 3:

$$\frac{T_{e(av)}k_{ins}^2}{\Delta x_{ins}^2 I\, h_f} = C_1^{'}\left(\frac{h_a \Delta x_{ins}}{k_{ins}}\right)^{-0.001} \tag{27}$$

Rearranging (26) and (27), then

$$C_1 = \frac{T_{e(av)}k_{ins}^2}{\Delta x_{ins}^2 I\, h_f}.\left(\frac{k_{ins}}{h_a \Delta x_{ins}}\right)^{-0.0001} \tag{28}$$

and

$$C_1^{'} = \frac{T_{e(av)}k_{ins}^2}{\Delta x_{ins}^2 I\, h_f}.\left(\frac{k_{ins}}{h_a \Delta x_{ins}}\right)^{-0.001} \tag{29}$$

Given the specificity of the data groups, the following constants are defined C_1, C_2 and C_3. The form of the dimensionless equations for the groups becomes

$$C_1 = \frac{T_{e(av)}k_{ins}^2}{\Delta x_{ins}^2 I\, h_f}.\left(\frac{k_{ins}}{h_a \Delta x_{ins}}\right)^{-0.0001}\Bigg|_{avg} = \frac{T_{e(av)}k_{ins}^2}{\Delta x_{ins}^2 I\, h_f}.\left(\frac{1}{Nu_{\Delta x_{ins}}}\right)^{-0.0001}\Bigg|_{avg} \tag{30}$$

$$C_2 = \frac{T_{e(av)}k_{ins}^2}{\Delta x_{ins}^2 I\, h_f}.\left(\frac{k_{ins}}{h_a \Delta x_{ins}}\right)^{-0.0001}\Bigg|_{avg} = \frac{T_{e(av)}k_{ins}^2}{\Delta x_{ins}^2 I\, h_f}.\left(\frac{1}{Nu_{\Delta x_{ins}}}\right)^{-0.0001}\Bigg|_{avg} \tag{31}$$

$$C_3 = \frac{T_{e(av)}k_{ins}^2}{\Delta x_{ins}^2 I\, h_f}.\left(\frac{k_{ins}}{h_a \Delta x_{ins}}\right)^{-0.001}\Bigg|_{avg} = \frac{T_{e(av)}k_{ins}^2}{\Delta x_{ins}^2 I\, h_f}.\left(\frac{1}{Nu_{\Delta x_{ins}}}\right)^{-0.001}\Bigg|_{avg} \tag{32}$$

The average values of the expressions contained in the last three equations are taken from Table 1 in order to obtain the values of the constants. Specifying the constraints for the respective groups defined by the $Nu_{\Delta x_{ins}}$ variables in the table, the following dimensionless equations are obtained:

for Group 1:

$$\frac{T_{e(av)}k_{ins}^2}{\Delta x_{ins}^2 I\, h_f} = 1.84\left(\frac{h_a \Delta x_{ins}}{k_{ins}}\right)^{-0.0001} \tag{33}$$

subject to the constraints

$$30 < Nu_{\Delta x_{ins}} < 300$$

for Group 2:

$$\frac{T_{e(av)} k_{ins}^2}{\Delta x_{ins}^2 I\, h_f} = 184 \left(\frac{h_a \Delta x_{ins}}{k_{ins}} \right)^{-0.0001} \tag{34}$$

subject to the constraints

$$0.06 < Nu_{\Delta x_{ins}} \leq 30$$

and for Group 3:

$$\frac{T_{e(av)} k_{ins}^2}{\Delta x_{ins}^2 I\, h_f} = 4.6 \times 10^7 \left(\frac{h_a \Delta x_{ins}}{k_{ins}} \right)^{-0.001}$$

subject to the constraints

(35)

$$0.006 < Nu_{\Delta x_{ins}} \leq 0.06$$

Notably, equation (33) is useful in determining the average edge temperature of the absorber in situations where excellent i lation is used. Considering the specified constraints, the second (34) is useful in cases where relatively poor edge insulation is used, and the third (35) where a conducting interface is employed, i.e. a metal-to-metal edge. The important benefit of predicting $T_{e(av)}$ from the condensed nondimensional equations is that once its value is known the edge heat loss from a flat plate absorber can be immediately determined, using equations (13) and (14).Also, by predicting $T_{e(av)}$, the amount of insulation needed to maintain a particular temperature at the edges of the absorber can be determined for specific design considerations, and also calculate the edge loss associated with a given insulation material for some prescribed operational variables, hence the thermal efficiency. The edge loss shows a strong dependence on the operational parameters, the effects of varying convective heat transfer coefficient h_f are examined as contour plots (Fig.3), which show visual and numerical differences. The equations which are given here are useful in calculating the effects of ambient parameters on the evolution of the absorber edge temperature, and determining the extent of the edge dissipation and the effectiveness of the insulation provision.

RESULTS AND DISCUSSION

The evolution of the nodal temperature values of the absorber with k_{ins} and T_a parameters are presented in Figures 3-5.The analysis is carried out to evaluate the effects of the parameters on the temperature profile of a typical flat-plate absorber. In the figures, it is seen that the nondimensional nodal temperature drops from a corresponding mid-node along a transverse nodal line to the exterior nodes, and also this drop is sideways owing to symmetrical loading conditions. It is seen that at T_a = 278K (Figure 4), the nondimensional nodal temperature values are a maximum for the plate with excellent insulation ($\bar{\kappa} = 1.67e-4$) with all nodes having equal values as a result of no edge loss. For increasing high $\bar{\kappa}$ values however, it is seen that the nodal temperature values rise from both edges of the absorber plate to the central node of any transverse nodal line due to the fact that poorly insulated edges have increased dissipation at the boundary edges than at the inner nodes. In Figure 5, a similar effect is observed but with reduced differences in the nodal values for various $\bar{\kappa}$ values. In Figure 6 a contrary result is seen, since T_a is relatively high heat is transferred from the surroundings to the plate with poor or no edge insulation hence the boundary nodes have higher values than the inner nodes for high $\bar{\kappa}$ values and the nodal values are highest for the plate without edge insulation. The significance of the changes in the temperature profile indicates that the ambient air temperature can affect the performance of poorly insulated solar air heaters or the heaters with no edge insulation at all. High ambient temperatures are good for poorly insulated absorbers however in situations where the ambient temperature is low, excellent insulation is needed. An empirical study on the effects of ambient temperature has been investigated [13], and is in agreement with the present analysis. Figures 7 and 8 give a clear indication in respect of the influence of the thermophysical property of the insulation and the geometric and ambient characteristics of the absorber on the thermal performance of the plate. As $\bar{A}_e$ increases the edge loss becomes very significant with high U_e values showing that high edge loss coefficient values characterized by high k_{ins} and h_a values affects the magnitude of the edge loss, especially in small absorbers. Results in Figure 8 show that as the dimensionless absorber plate

temperature $\bar{T}_p$ increases with U_e , φ_{edge} increases also, emphasizing that absorbers with poor edge insulation and high ambient temperatures have increase edge heat dissipation. It is seen that if an absorber with high surface temperatures and no edge insulation is in an environment characterized by high h_a and relatively low T_a, the edge loss will be very significant as given by the plots of the plate without edge insulation (figures 7 and 8).Hence, in heat transfer processes involving a flat-plate absorber with heat dissipation at the edges, the influence of high $\bar{A}_e$ and $\bar{T}_p$ ratios must be carefully considered for superior performance. In typical applications however where the edge loss is not desired, adequate insulation provision should be made. It can be deduced that as $k_{ins} \to \infty$ and $\Delta x_{ins} \to 0$, the edge loss coefficient $U_{edge} \to h_a$.

Equation (14) therefore gives the theoretical limit for the case. Plots 9, 10 and 11 show the different operating regimes of the absorber with respect to the $Nu_{\Delta x_{ins}}$ parameters. In figure 8 showing results of group 1,the operating regime of the Nusselt number is between 30 and 300.For group 2, the operating range of the Nusselt number is between 0.006 and 30. And for group 3, the range is between 0.006 and 0.06.The dependence of the average edge temperature of an absorber on the heat transfer coefficient for a case of constant heat flux and thermophysical properties, can be expressed as

$$T_{e(av)} \alpha \; h_a^n \tag{36}$$

where $n = -1$ for an equation of the form of Newton's law of cooling. But for the average edge temperature of the absorber with insulation, n is in the range of -0.001 to -0.0001.This is much weaker than the value of n found in [14, 15], the main reason for this is that more data points were used and the effects of thermal interaction in the system were incorporated into the equations. The correlation is congruent with the Newton's law of cooling [14] when plotted considering the variables above, and conforms to results obtained in [13, 16] where the effects of convective heat transfer coefficient on the thermal performance of a solar absorber were investigated. From the plots, the average edge temperature of the absorber can be immediately determined if the other parameters are known. The Nusselt number gives the ratio of the convective heat transfer coefficient to conduction in the insulation. The plot in figure 9 can be useful in determining the average absorber temperature in situations where excellent insulation is used. The plot in figure 10 is applicable where relatively poor

insulation is employed, and that of figure 11 is applicable to a conducting interface. The important benefit of predicting $T_{e(av)}$ from the condensed plots is that once its value is known the edge heat loss can be immediately determined, using equations (13) and (14).

Conclusion

Some unique dimensionless parameters were identified for the edge loss in flat plate absorbers employing real-world conditions. Prediction equations based on these dimensionless parameters were also determined for various operating conditions of the absorber. The dimensionless edge heat loss equation obtained here can be of important benefit in making predictions of the influence of ambient and the use parameters on the thermal performance of flat-plate absorbers, as well as calculating the edge heat transfer rate, especially for absorbers with high A_e/A_p ratios with considerable edge heat dissipation. Also, it is seen that proper edge insulation improves steady-state heat transfer and equalizes temperatures over the absorber-plate. This is particularly useful in the design of small energy conversion devices, and thermo-electric components with impinging radiation.

Nomenclature

A – *Area of a differential* (m^2)

A_e – *Absorber plate edge area* (m^2)

A_p – *Absorber plate area* (m^2)

h – *Convective heat transfer coefficient* $\left(\frac{W}{m^2 K}\right)$

I – *Incident (hourly) solar radiation intensity* $\left(\frac{W}{m^2}\right)$

k – *Thermal conductivity* $\left(\frac{W}{mK}\right)$

L – *Length of absorber – plate* (m)

M – *Number of element*

Q – *Heat transfer* (W)

$q_{e_{loss}}$ – *Edge conduction heat flux* $\left(\frac{W}{m^2}\right)$

T – *Temperature* (K)

T_i – *Temperature at node* i (K)

t – *Thickness of the absorber – plate* (m)

U – *Heat loss conductance* $\left(\frac{W}{m^2}\right)$

W – *Width of absorber – plate* (m)

Greek symbols

ΔT – *Temperature difference* (K)

Δx_{ins} – *Thickness of insulation material* (m)

Ω_{edge} – *Element periphery* (m)

α – *Solar absorptivity of coating*

τ – *Overall transmissitivity of transparent cover plates*

Subscripts

a – *Ambient air*

av – *Average*

e – *edge*

f – *The working fluid*

i – *Node number*

ins – *Insulation – outer frame interface*

t – *top*

x – *x direction*

y – *y direction*

References

1. H.P. Garg, C. Ram, R. Usha, Transient Analysis of Solar Air Heaters Using Finite Difference Technique, International Journal of Energy Research 1981,Volume 5,Pages 243-252.
2. S.A. Kaligrou, Solar Energy Engineering Processes and Systems, Elsevier, pp.156-163, 2009.\
3. J. A. Duffie, and W. A. Beckman, Solar Engineering of Thermal Processes, Wiley & Sons Inc, New York, 1991.
4. B. Chambers and T. L.Tien-Yu, A Numerical Study of Local and Average Natural Convection Nusselt Numbers for Simultaneous Convection Above and Below a Uniformly Heated Horizontal Thin Plate, Journal of . Heat Transfer 119,Iss.1, 102-108,1997.
5. M.K. Gupta and S.C. Kaushik, Performance evaluation of solar air heater having expanded metal mesh as artificial roughness on absorber plate , International Journal of Thermal Sciences, Volume 48, Issue 5, May 2009, Pages 1007-1016.
6. L. Harikrishnan, Shaligram Tiwari, and M.P. Maiya, Numerical study of heat and mass transfer characteristics on a falling film horizontal tubular absorber for R-134a-DMAC, International Journal of Thermal Sciences, Volume 50, Issue 2, February 2011,Pages149-159.
7. Njomo, D.; Daguenet, M. Sensitivity analysis of thermal performances of flat plate solar air heaters. Journal of Heat and MassTransfer 2006, 42, 1065–1081..
8. Champion, E.R., Jr. Finite Element Analysis in Manufacturing Engineering: A PC-Based Approach; McGraw Hill: New York, 1992
9. Hilton, D.V. Fundamentals of Finite Element Analysis; McGraw Hill:New York, 2004.
10. C. B. Sohann, and S.V. Garimella, “A Comparative Analysis on Studies of Heat Transfer and Fluid flow in Microchannels,” Microscale thernophys. Eng., 5,pp. 293-311,2001,.
11. P.N. Nwosu, Edge Convection Heat Loss analysis in a Solar Air Heater Using Finite Element Method,Ph.D Thesis, University of Nigeria,Nsukka,2011.
12. Janna S.W., Introduction to Fluid Mechanics, 3rd Edition 168-176, 1993.

13. S. Janjai, P. Tung, Performance of a Solar Dryer Using Hot air from roof-integrated Solar Collectors for Drying Herbs and Spices, Renewable Energy, Volume 30,Issue 14,Pages 2085-2095,2006.
14. F.P. Incropera, T. L. Bergman, A. S. Lavine, D. P. DeWitt,Fundamentals of Heat and Mass Transfer, John Wiley & Sons, 2011
15. F. Kern, S.M. Bohn, Principles of Heat Transfer, Harpes and Row, New York; 1992.
16. R. J. Kind, D. H. Gladstone, and A. D. Moizer, Convective Heat Losses From Flat-Plate Solar Collectors in Turbulent Winds, J. Sol. Energy Eng., Volume 105, Issue 1, pp. 80-85

Figures

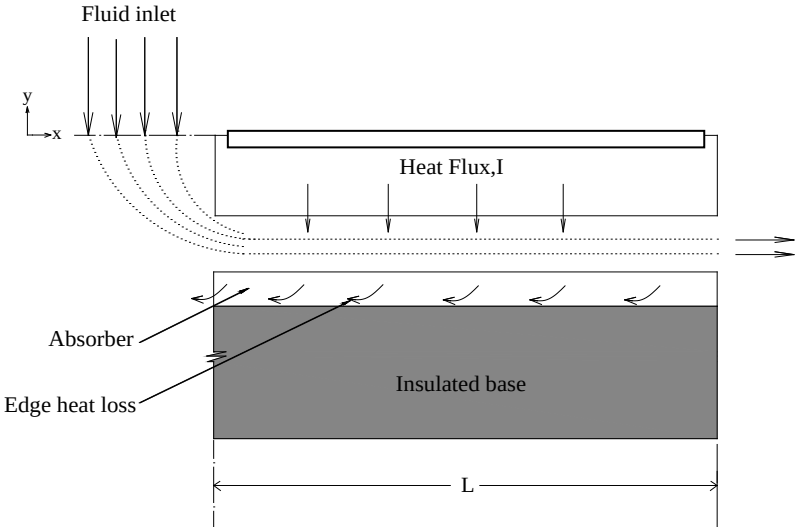

Figure 1: Nomenclature of the problem

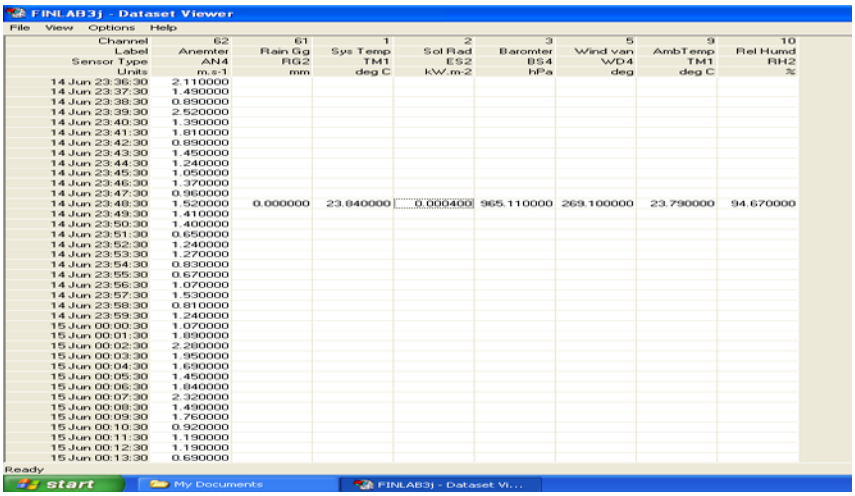

Figure 2: A view of DataSet weather logger

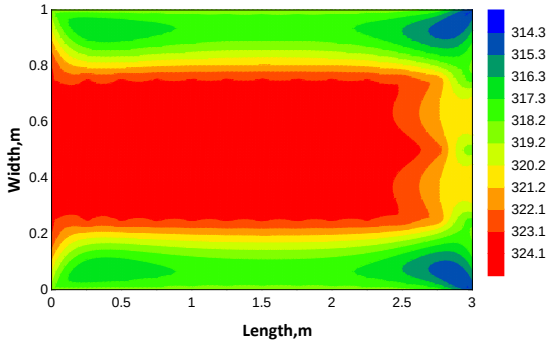

(a)

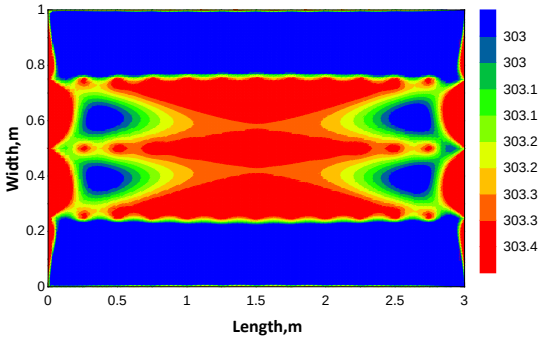

(b)

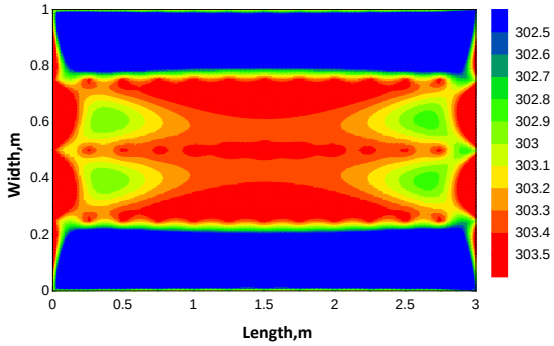

(c)

Figure 3: Contours of temperature for an absorber with no edge insulation: (a) h_f = 5 W/m^{2}K; (b) h_f = 50 W/m^{2}K;(c) h_f =100 W/m^{2}K

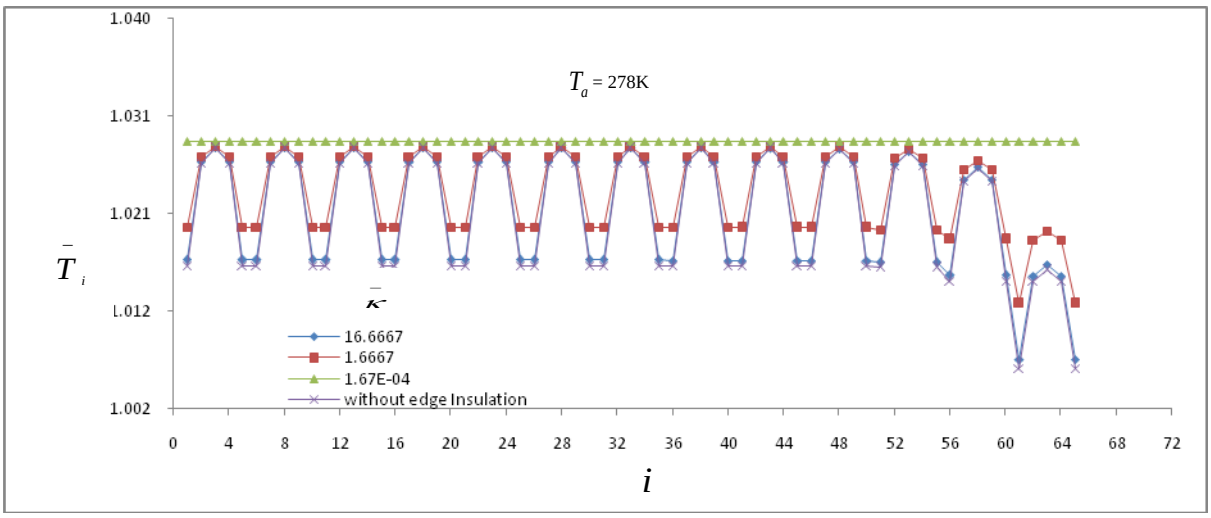

Figure 4: Nondimensional temperature profile of the absorber with varying insulation values for T_a = 278K

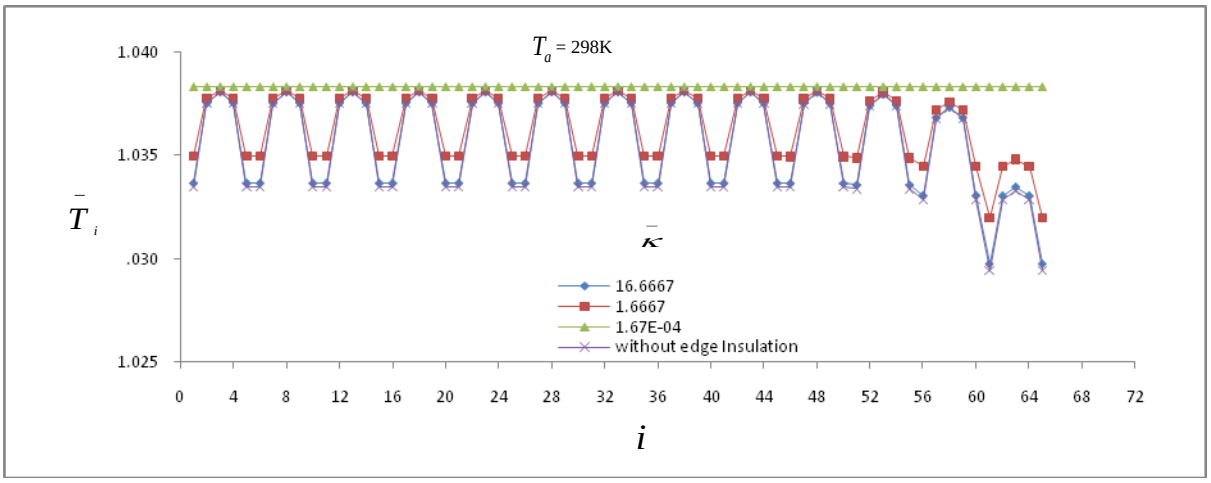

Figure 5: Nondimensional temperature profile of the absorber with varying insulation values for T_a = 298K

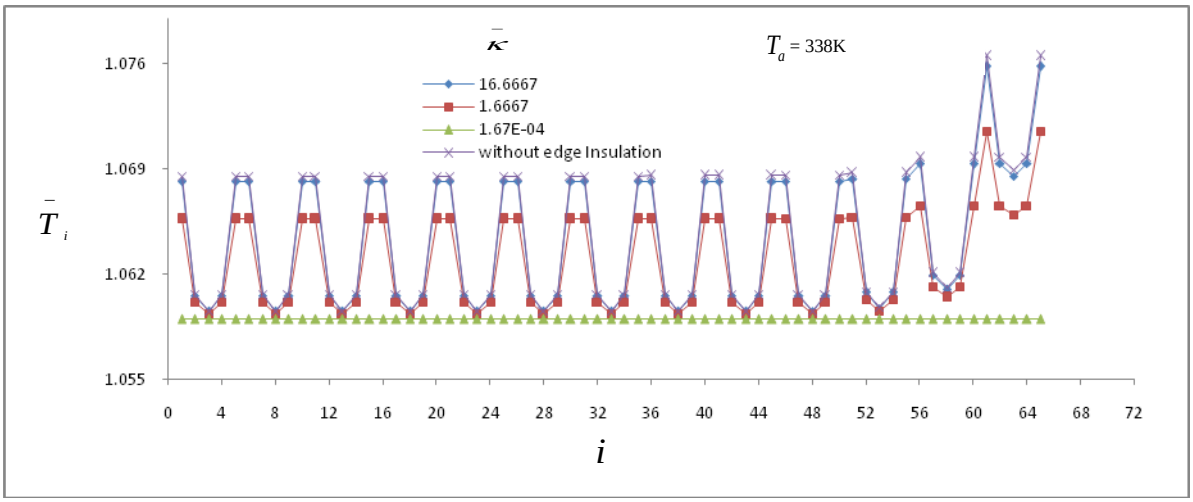

Figure 6: Nondimensional temperature profile of the absorber with varying insulation values for T_a = 338K

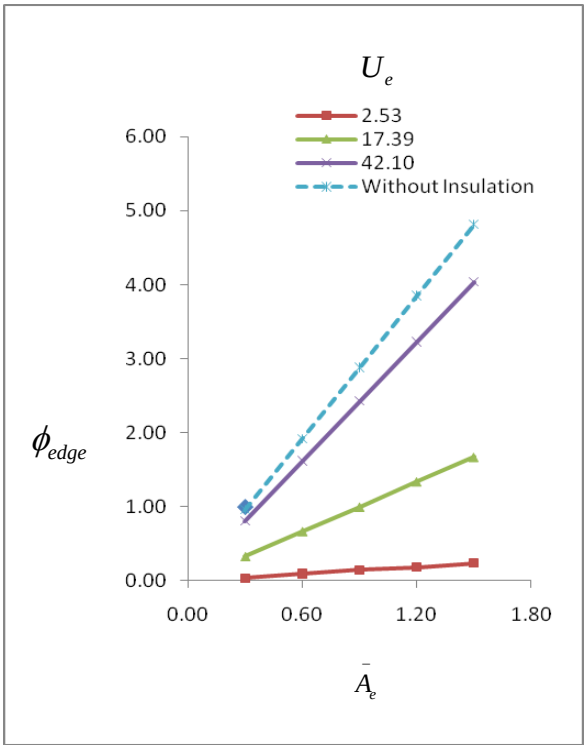

Figure 7: Evolution of ϕ_{edge} with U_e in relation to varying A_e values

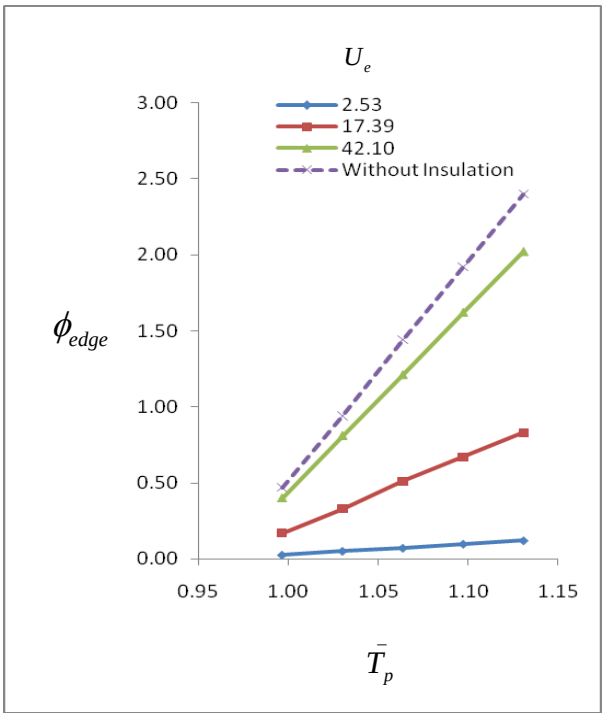

Figure 8: Evolution of ϕ_{edge} with U_e in relation to varying $\bar{T}_p$ values

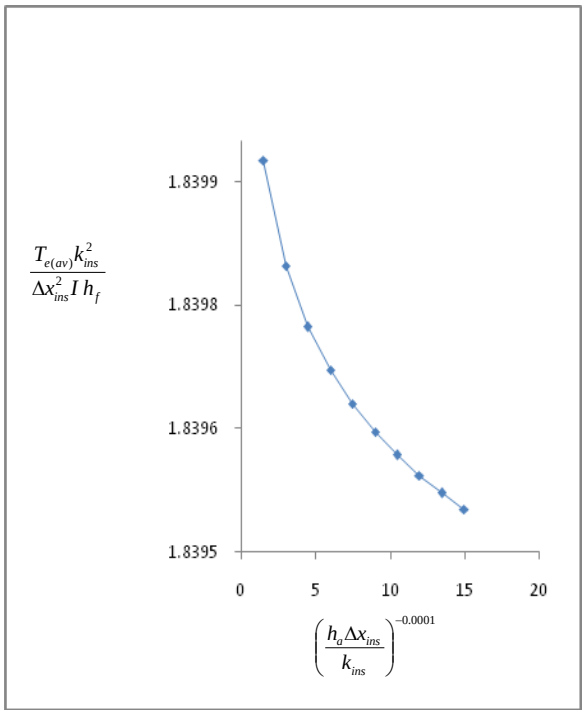

Figure 9: Plots of the nondimensional groups for the range $30 < Nu_{\Delta x_{ins}} < 300$

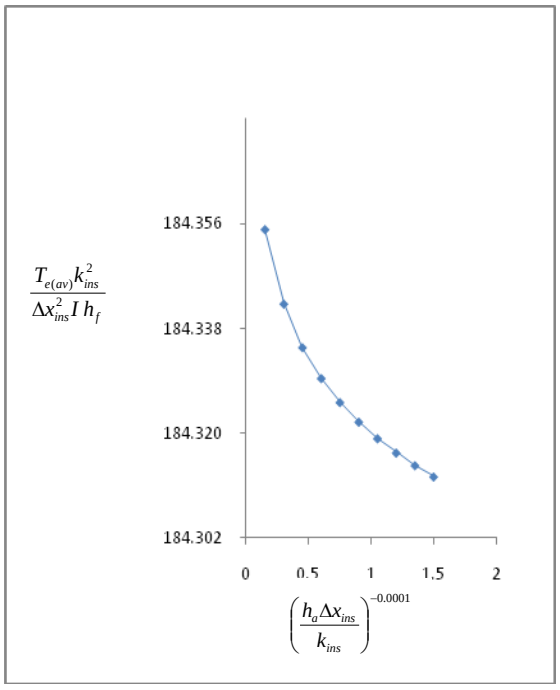

Figure 10: Plots of the nondimensional groups for the range $0.06 < Nu_{\Delta x_{ins}} \leq 30$

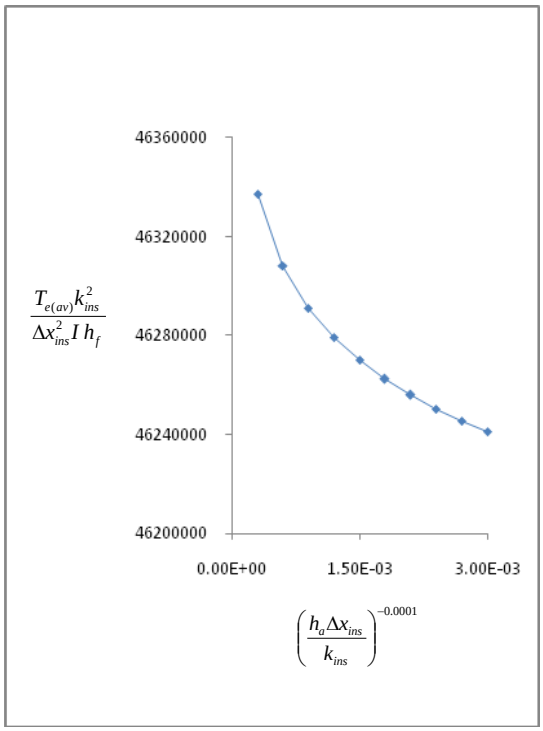

Figure 11: Plots of the nondimensional groups for the range $0.006 < Nu_{\Delta x_{ins}} \leq 0.06$

Table 1: Model Results for $T_{e(av)}$ and the non-dimensional equations

Run	$T_{e(av)}(K)$	$h_a\left(W/m^2K\right)$	$T_{e(av)}k_{ins}^2/It_{ins}^2h_f$	h_at_{ins}/k_{ins}	k/k_{ins}	$k_{ins}T_a/t_{ins}I$	$k_{ins}T_f/t_{ins}I$	$\left(T_{e(av)}k_{ins}^2/It_{ins}^2h_f\right)\left(h_at_{ins}/k_{ins}\right)^{-1}$	a^3
Group 1									
1	311.1494675	10	1.843848696	1.5	10000	4.04	4.04	1.843923459	
2	311.0849153	20	1.843466164	3	"	"	"	1.843668701	
3	311.0611595	30	1.843325389	4.5	"	"	"	1.843602661	
4	311.0488121	40	1.84325222	6	"	"	"	1.843582516	
5	311.0412463	50	1.843207385	7.5	"	"	"	1.843578811	
6	311.036135	60	1.843177096	9	"	"	"	1.843582128	
7	311.0324506	70	1.843155263	10.5	"	"	"	1.843588709	
8	311.0296687	80	1.843138777	12	"	"	"	1.843596837	
9	311.0274939	90	1.84312589	13.5	"	"	"	1.843605661	
10	311.025747	100	1.843115538	15	"	"	"	1.84361473	
							Average	1.843634421	-0.0001
Group 2									
1	311.1351545	10	184.3763879	0.15	1000	40.4	40.4	184.3414128	
2	311.0685177	20	184.3368994	0.3	"	"	"	184.314707	
3	311.0439359	30	184.3223324	0.45	"	"	"	184.3076147	
4	311.0311455	40	184.3147529	0.6	"	"	"	184.3053379	
5	311.0233034	50	184.3101057	0.75	"	"	"	184.3048035	
6	311.0180033	60	184.3069649	0.9	"	"	"	184.3050231	
7	311.0141817	70	184.3047003	1.05	"	"	"	184.3055995	
8	311.0112957	80	184.30299	1.2	"	"	"	184.3063503	
9	311.0090391	90	184.3016528	1.35	"	"	"	184.3071838	
10	311.0072262	100	184.3005785	1.5	"	"	"	184.3080514	
							Average	184.3106084	-0.0001
Group 3									
1	311.0866368	10	46086909.16	0.0003	2	20200	20200	45751674.32	
2	310.9606593	20	46068245.83	0.0006	"	"	"	45761685.47	
3	310.8772378	30	46055887.08	0.0009	"	"	"	45766106.82	
4	310.8068554	40	46045460.05	0.0012	"	"	"	45767593.73	
5	310.7428064	50	46035971.32	0.0015	"	"	"	45767352.76	
6	310.6826977	60	46027066.33	0.0018	"	"	"	45766008.82	
7	310.625441	70	46018583.86	0.0021	"	"	"	45763923.11	
8	310.570456	80	46010437.92	0.0024	"	"	"	45761321.43	
9	310.5173941	90	46002576.91	0.0027	"	"	"	45758353.33	
10	310.4660264	100	45994966.88	0.003	"	"	"	45755122.2	
							Average	45761914.2	-0.001

Parameters:	$k=100W/mK$	$T_a=303K$	$t=0.0015m$	$T_f=303K$	$I=500W/m^2$	$h_f=15W/m^2K$
	k_{ins} :	Group 1 0.01 W/mK	Group 2 0.10 W/mK	Group 3 50.0 W/mK		